Scanning Microscopy

Volume 2 | Number 3 Article 16

7-10-1988

Contribution of Densely Distributed Electron Beam Induced Current Contrasts in Annealed Cz Silicon to Bulk Recombination

M. Kittler
Academy of Sciences of the GDR Institute of Semiconductor Physics

W. Seifert
Academy of Sciences of the GDR Institute of Semiconductor Physics

Scanning Microscopy, Vol. 2, No. 3, 1988 (Pages 1397-1406)
Scanning Microscopy International, Chicago (AMF O'Hare), IL 60666 USA

0891-7035/88$3.00+.00

CONTRIBUTION OF DENSELY DISTRIBUTED ELECTRON BEAM INDUCED CURRENT CONTRASTS IN ANNEALED CZ SILICON TO BULK RECOMBINATION

M. Kittler* and W. Seifert

Academy of Sciences of the GDR
Institute of Semiconductor Physics
1200 Frankfurt (Oder), G.D.R.

(Received for publication February 24, 1988, and in revised form July 10, 1988)

Abstract

The paper presents a detailed analysis of Electron Beam Induced Current (EBIC) diffusion-length and contrast data for samples containing defect accumulations. The formulae given allow one to estimate to which extent the average diffusion length is determined by recombination-active defects showing EBIC contrast.

This analysis may be used to identify essential sources of bulk recombination in annealed silicon. In the light of our results stacking faults are an essential source of bulk recombination in intrinsically gettered p-type Cz silicon.

KEY WORDS: Diffusion Length, Electron Beam Induced Current, Carrier Recombination, Crystal Defects, Intrinsic Gettering, Silicon, Semiconductor Characterization.

*Address for correspondence:
Akademie der Wissenschaften der DDR
Institut für Halbleiterphysik
W.-Korsing-Str. 2, Frankfurt (Oder),
DDR -1200 Phone No: 3730

Introduction

Intrinsic gettering (IG) procedures in Cz silicon result in the formation of a depth-dependent concentration of defects characterized by a low density of crystal defects at the surface (denuded zone) and a high defect density in the wafer bulk. Thereby, the bulk defects are important as gettering sites for undesired impurities /15/. The profile of defect density leads to a corresponding profile of recombination properties (recombination lifetime τ_R respectively diffusion length L), with low recombination in the denuded zone and strong recombination in the bulk (Fig. 1).

Although devices are usually located in the highly perfect denuded zone the bulk region is not unimportant for device operation /16,10/. Accordingly, there is an interest in characterizing bulk recombination and its sources. This knowledge is a necessary prerequisite for lifetime engineering.

The EBIC method is well suited for investigating the sources of bulk recombination as it allows both to image and investigate the recombination-active crystal defects in a certain area of a sample and to determine the average diffusion length in the same sample area. An example for an EBIC image of volume defects in annealed Cz silicon is given by Fig. 2a.

It is obvious that such crystal defects showing dark EBIC contrasts reduce the average diffusion length in the material because dark contrasts indicate additional recombination. However, crystal defects having EBIC contrast are not the only causes of bulk recombination.

Other crystal defects not resolvable by EBIC due to their low recombination activity and/or their high density and point defects may also contribute to bulk recombination (Fig. 2b). So, to a first approximation the resulting average diffusion length in the bulk of the sample,

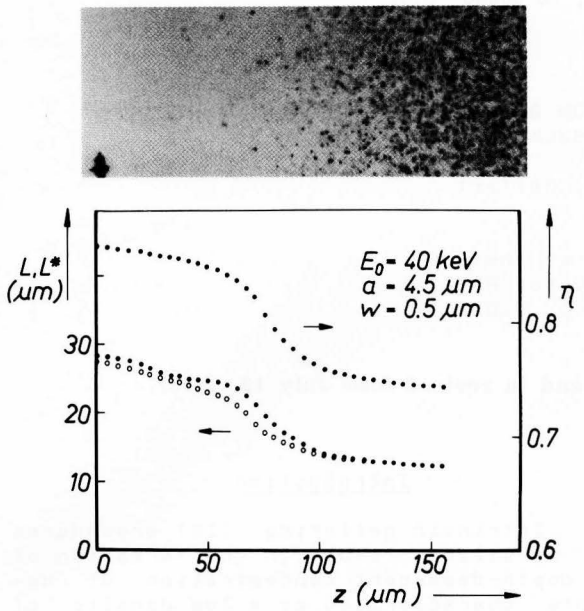

Fig. 1. EBIC micrograph of a bevelled IG-sample ($\alpha \simeq 3.5^{\circ}$) taken at $E_0 = 30$ keV and related depth profiles of the charge collection efficiency η (•), effective diffusion length L* (o) and true diffusion length L (•), for detailed information see /3/.

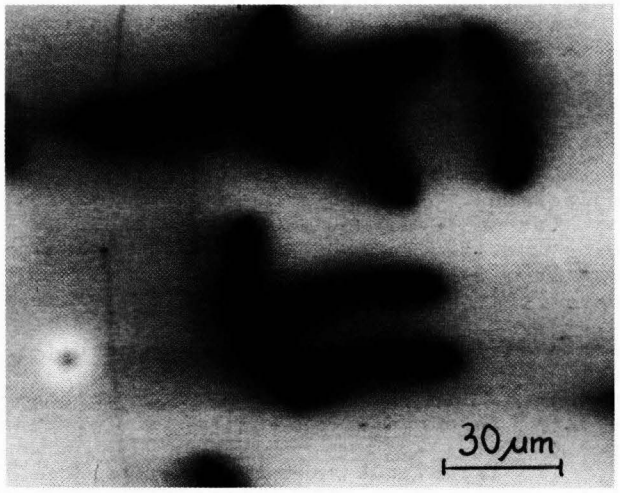

Fig. 3. Dark EBIC contrasts at stacking faults and bright EBIC halo around a point-like defect (p-type silicon, Al Schottky diode, $E_0 = 25$ keV).

L_B, is given by:

$$L_B^{-2} = L_E^{-2} + L_M^{-2} \qquad (1)$$

with L_E describing the contribution of the observed defects with EBIC contrasts

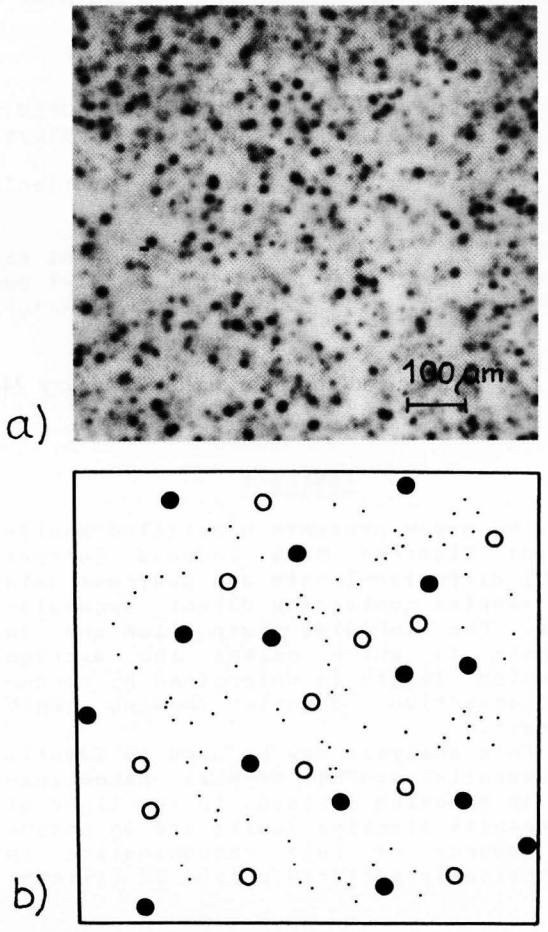

Fig. 2. Volume defects in annealed Cz silicon.
a) EBIC micrograph of an annealed sample (p-type silicon, Al Schottky contact, $E_0 = 30$ keV).
b) Schematic illustration of the different defect types contained in a sample: Defects having EBIC contrast (full circles) define the diffusion-length component L_E while point defects (points) and extended defects giving no EBIC contrast (open circles) determine the component L_M.

and L_M the contribution of the surrounding material being due to point defects and crystal defects without contrast (recombination background).

L_B can be determined directly by energy-dependent charge collection measurements $\eta(E_0)$ /17,9/, while L_E could be estimated from contrast data /8/:

$$L_E \simeq \lambda \left(\frac{R\, f_{max}}{c_{max}}\right)^{1/2} \qquad (2).$$

λ is the average distance between EBIC contrasts, c_{max} the maximum EBIC contrast

in the sample area investigated, R the electron range /5/ at the beam energy E_o used for imaging and f_{max} a correction factor to be calulated - for more detailed information on c and f see below.

Application of relation (2) to experimental data proved to yield quite satisfactory results, e. g., $L_E > L_B$ in all cases as required by (1) /8/.

The present paper proves relation (2) given for accumulations of EBIC contrasts and discusses experimental investigations of closely neighboured crystal defects in annealed Cz silicon using relations (1) and (2).

Description of the EBIC contrast at individual defects

The EBIC contrast function $c(\vec{r})$ of an isolated defect is defined by:

$$c(\vec{r}) = 1 - \frac{I(\vec{r})}{I_o} \qquad (3).$$

$I(\vec{r})$ and I_o are the beam-induced currents collected at arbitrary beam position $\vec{r}$ and at beam positions sufficiently far from the defect, respectively. Thereby, both positive (dark) and negative (bright) contrasts may be found in practice - see Fig. 3.

Positive contrast caused by enhanced carrier recombination at defects is the most important contrast type and can be well described by existing theoretical models /2,13/.

Such positive recombination contrasts only will be discussed below. According to Donolato /2/ the contrast function due to a point-like recombination-active defect in the neutral semiconductor may be written as /11/:

$$c(\vec{r}) = \gamma\, f(\vec{r}) \qquad (4).$$

γ is the recombination strength of the defect (having dimension of a length in our notation) and is related to the number of recombination centres, n, at the defect and their effective capture cross section, σ, by /11/:

$$n\sigma = \gamma \frac{D}{V_{th}} \qquad (5)$$

with D being the minority carrier diffusivity and V_{th} their thermal velocity.

$f(\vec{r})$ is given in /2/ and represents a correction function depending on defect depth, diffusion length L_M in the material surrounding the defect, electron probe position $\vec{r}$, and primary electron range R. When the electron beam is positioned just above a given defect the correction function is at its largest value f_d and the contrast is given by:

$$c = \gamma f_d \qquad (4').$$

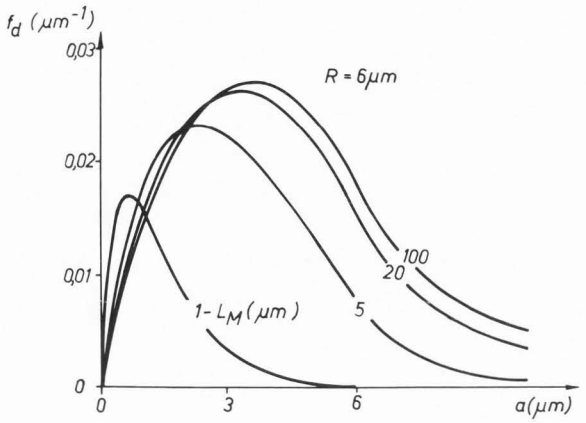

Fig. 4. Correction factor of a point-like defect, f_d, versus defect depth, a, calculated for R = 6 μm, with the diffusion length L_M as parameter, see also /12/.

Fig. 4 shows an example of a correction factor f_d of a point-like defect, for more detailed information see also /12/. At sufficiently large L_M the correction factor f_d becomes nearly independent of L_M and at R = 6 μm the maximum correction factor becomes $f_{max} \simeq 0.027\ \mu m^{-1}$ for a defect depth of a ≃ 4 μm. Correction factors for line-shaped defects, e. g., dislocations, can be found in /4, 12/.

The EBIC collected near an isolated defect, $I(\vec{r})$, may be written:

$$I(\vec{r}) = I_o\left[1 - \gamma f(\vec{r})\right] \qquad (6).$$

Similarly, the EBIC obtained with the electron beam positioned above the defect, I_d, is given by:

$$I_d = I_o\left[1 - \gamma f_d\right] \qquad (6').$$

Description of densely distributed EBIC contrasts and their contribution to bulk recombination

If we have an accumulation of closely neighbouring defects the resulting EBIC signal will be, of course, influenced by all of them. So, the EBIC current around a defect of strength γ located in a cloud of N other defects

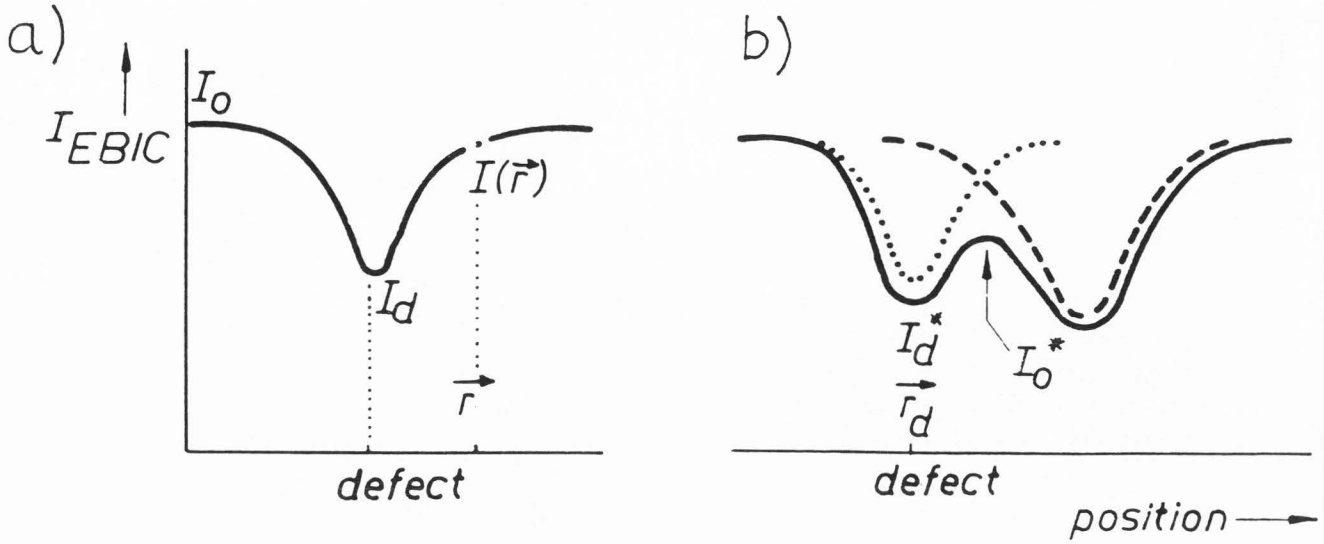

Fig. 5. EBIC distribution around point-like recombination-active defects;
a) isolated defect
b) defect with a close neighbour: (---), (...) EBIC profiles of the two contributing defects
(——) resulting EBIC distribution

is given by:

$$I^*(\vec{r}) = I_0\left\{1-\left[\gamma f(\vec{r}) + \sum_{i=1}^{N}\gamma_i f_i(\vec{r})\right]\right\} \qquad (7).$$

In Fig. 5 this influence is illustrated schematically for two closely neighbouring defects. Due to the superposition of the defect contrast functions the EBIC signal at the defect position $\vec{r} = \vec{r}_d$ is I_d^* instead of I_d and the maximum EBIC appearing between the defects is I_0^* instead of I_0.

Nevertheless, it can be shown that for defect distances well above the electron range R and for not too large defect strengths the contrast of such defects, c^*, is nearly equal to the contrast c of an isolated defect (unpublished result), i. e.,

$$c \simeq c^* \qquad (8).$$

This relation entitles us to treat the contrasts as contrasts of isolated defects in many cases of practical interest.

The property $c \simeq c^*$ will be used now to prove formula (2) relating the diffusion-length component due to EBIC contrasts, L_E, to EBIC contrast data (maximum contrast c_{max}, average distance between contrasts λ). Assume a homogeneous defect density depth-distribution F(a) (Fig. 6a), and a homogeneous defect-strength distribution $P(\gamma)$ up to a certain maximum defect strength γ_{max} (Fig. 6b).

In Fig. 7 the contrasts of these defects as calculated from (4') are shown in dependence on defect depth, a, with defect strength γ as parameter. The lower curve is the curve for the minimum defect strength γ_{min} still able to produce a visible contrast, the upper curve represents contrast versus depth for the maximum defect strength γ_{max}, and the dashed curve is for an intermediate defect strength $\gamma(a)$. Thereby, the following relations hold:

$$\gamma_{max} = \frac{c_{max}}{f_{max}}\,,\ \gamma_{min} = \frac{c_{min}}{f_{max}}\,,\ \gamma(a) = \frac{c_{min}}{f(a)} \qquad (9).$$

The shaded area in Fig. 7 defines the portion of defects having visible EBIC contrast, i. e., $c_{min} \leq c \leq c_{max}$. Defects at depth between a_u and a_l only can be observed. The so defined information range $\Delta a = a_l - a_u$ depends on c_{min} and c_{max}, with $\Delta a < R$ for $c_{min}/c_{max} \to 1$ and $\Delta a > R$ for $c_{min}/c_{max} \ll 1$ (see Fig. 8).

To estimate the recombination component due to visible defects we treat all the recombination centres located at the defects as being distributed homogeneously in the depth interval Δa in which contrasts can be observed. So we may write:

$$L_E^{-2} = \frac{1}{\tau_E D} = \frac{1}{\Delta a}\frac{v_{th}}{D}\sum_i (n\sigma)_i \qquad (10)$$

as for homogeneous distributions of cen-

tres. $(n\sigma')_i$ is the product of capture cross-section and number of centres at the i-th defect and the sum includes all visible defects per unit area. As:

$$(n\sigma')_i = \gamma_i \frac{D}{v_{th}} \quad \text{, see (5),}$$

the defect component of the diffusion length L_E is simply given by:

$$L_E^{-2} = \frac{1}{\Delta a} \sum_i \gamma_i \qquad (11)$$

with $\Sigma \gamma_i$ as strengths sum of all visible defects per unit area.

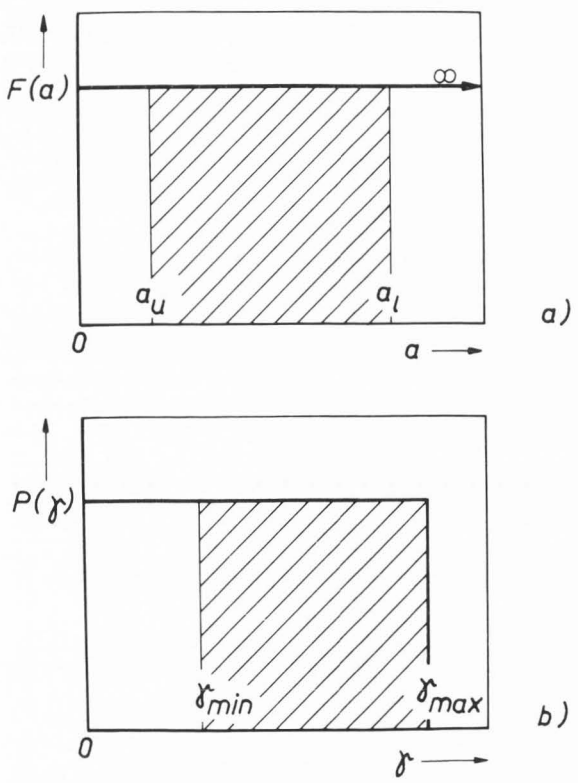

Fig. 6. Assumptions about defects;
a) depth distribution: constant defect density (defect number per unit area and per depth elements) F(a) versus depth a
b) strength distribution: existence of a maximum defect strength γ_{max} and equal probability $P(\gamma) = \gamma_{max}^{-1}$ for all γ between 0 and γ_{max}.
The shaded areas define the range of defect depths and defect strengths, respectively, where defects may be observed.

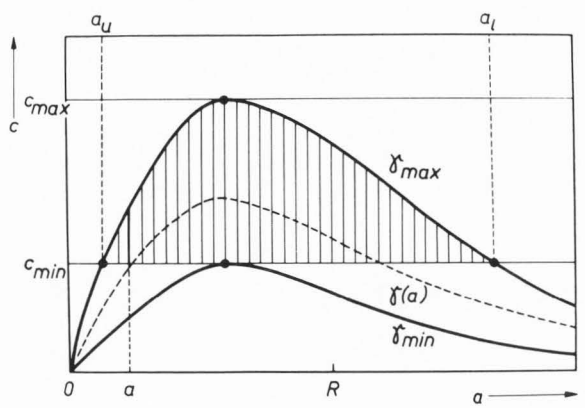

Fig. 7. Schematic drawing of contrast, c, versus defect depth, a, with defect strength γ as parameter.

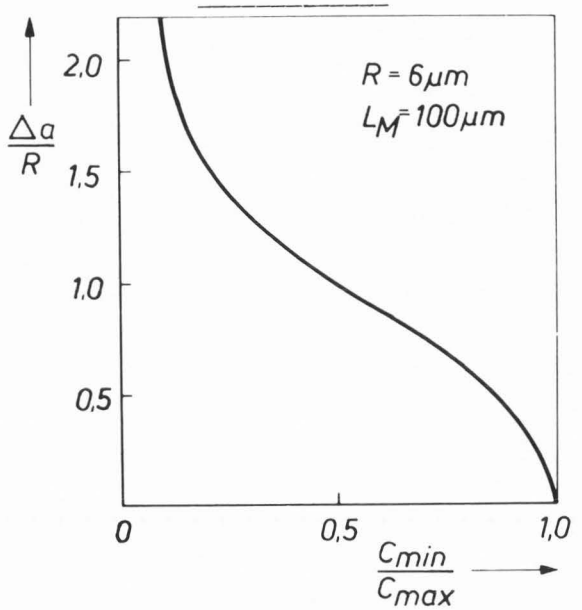

Fig. 8. Normalized depth range where defects may be observed, $\Delta a/R = (1/R)(a_l - a_u)$, versus contrast ratio c_{min}/c_{max} for R = 6 μm and L_M = 100 μm.

According to the assumed depth and strength distributions (Figs. 6a and b) of defects the sum $\Sigma \gamma_i$ is now replaced by a double integration. Thereby defect visibility requires contrasts larger than c_{min} and defines the integration limits (limits set on visibility by the spatial resolution of the EBIC method are not taken into account here). We obtain:

$$L_E^{-2} = \frac{1}{\Delta a} \int_{a_u}^{a_l} F(a) \left[\int_{\gamma(a)}^{\gamma_{max}} P(\gamma)\, \gamma \, d\gamma \right] da \qquad (12)$$

where $\gamma(a) = c_{min}/f(a)$ is the minimum γ for a given defect depth a which still produces a visible contrast and a_u and a_1 define the depth range where contrast can be observed (compare Fig. 7).
Using (9), $x = \Delta a/R$, and the distribution functions $P(\gamma)$ and $F(a)$ given in Fig. 6 integration leads to the following result:

$$L_E^2 = 2\,\frac{xR\,f_{max}}{F(a)c_{max}}\left\{\int_{a_u}^{a_1}\left[1-\left(\frac{c_{min}}{c_{max}}\frac{f_{max}}{f(a)}\right)^2\right]da\right\}^{-1} \quad (13).$$

It is, however, useful to rewrite this formula once more using instead of F(a) the mean distance between contrasts, λ, which is determined directly from EBIC investigations.

As the square of λ is defined as the inverse of the number of visible defects per unit area we have:

$$\frac{1}{\lambda^2} = \int_{a_u}^{a_1} F(a)\left[\int_{\gamma(a)}^{\gamma_{max}} P(\gamma)\,d\gamma\right]da = F(a)\int_{a_u}^{a_1}\left[1-\frac{c_{min}}{c_{max}}\frac{f_{max}}{f(a)}\right]da \quad (14).$$

Inserting (14) into (13) we get the final result for the diffusion length component due to EBIC contrasts:

$$L_E = \lambda\left(\frac{R\,f_{max}}{c_{max}}\right)^{1/2}\sqrt{2\times\frac{\int_{a_u}^{a_1}\left[1-\frac{c_{min}}{c_{max}}\frac{f_{max}}{f(a)}\right]da}{\int_{a_u}^{a_1}\left[1-\left(\frac{c_{min}}{c_{max}}\frac{f_{max}}{f(a)}\right)^2\right]da}} \quad (15).$$

The left part at the right side of (15) is identical with relation (2), but the additional terms under the root introduce corrections depending on c_{min}/c_{max}.

This effect of the c_{min}/c_{max} ratio on the L_E value to be determined is illustrated below for two extreme cases:
(i) $c_{min}/c_{max} = 0.1$, i. e., very sensitive EBIC detection electronics or strong defects and
(ii) $c_{min}/c_{max} = 0.9$, i. e., poor sensitivity or weak defects. $R = 6\,\mu m$ and $L_M = 100\,\mu m$ are assumed.

One obtains:

$$L_E\left(\frac{c_{min}}{c_{max}}=0.1\right) = 1.8\,\lambda\left(\frac{R\,f_{max}}{c_{max}}\right)^{1/2}$$
$$L_E\left(\frac{c_{min}}{c_{max}}=0.9\right) = 0.5\,\lambda\left(\frac{R\,f_{max}}{c_{max}}\right)^{1/2} \quad (16).$$

Looking at (16) one should not conclude that L_E increases with decreasing c_{min}/c_{max} because at the same time the mean contrast distance λ decreases (see formula (14)). Using (13) one finds:

$$\frac{L_E\left(\frac{c_{min}}{c_{max}}=0.9\right)}{L_E\left(\frac{c_{min}}{c_{max}}=0.1\right)} \simeq 2$$

for $R = 6\,\mu m$ and $L_M = 100\,\mu m$. So we see that L_E depends weakly on the sensitivity of the electronics used.

The above results allow one to conclude that relation (2) may be used for a rough estimation of L_E, especially for usual c_{min}/c_{max} ratios. Improvements of the estimate are possible when applying formula (15).

Dependence of bulk diffusion length on mean distance between EBIC contrasts

Fig. 9 shows the average bulk diffusion length, L_B, versus mean distance between EBIC contrasts, λ, as calculated for an electron range $R = 6\,\mu m$ from (1) and (2). The diffusion length, L_M, arising from the recombination background and the maximum EBIC contrast, c_{max}, are taken as parameters. If $L_M \to \infty$ (background recombination missing) L_B is seen to increase linearly with λ, with a slope determined by the value of the EBIC contrast c_{max}. For finite L_M (existing recombination background), on the other hand, $L_B \to L_M$ is found for large λ.

Experimental investigations on densely distributed EBIC contrasts in annealed Cz silicon and discussion

Many different Cz silicon samples of the following characteristics were studied:
p-type, boron-doping, $\varrho = 10...20$ ohmxcm, 76 mm or 100 mm in diameter, (100) or (111) orientation, different contents of metallic impurities like Fe, Cu, Au, different oxygen content ($5...10 \times 10^{17}$ cm^{-3}), different heat treatments for IG (multistep heat treatments or ramping for nucleation, see e. g. /15/).

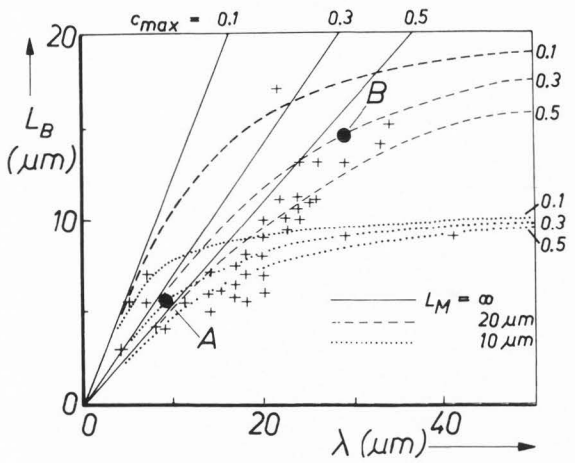

Fig. 9. Bulk diffusion length L_B versus mean distance λ between EBIC contrasts: Calculated curves for R = 6 μm (i. e., $E_o \simeq 28.5$ keV corresponding to /5/) with EBIC defect contrast, c_{max}, and diffusion-length component of the recombination background, L_M, as parameters, together with data measured at E_o = 30 keV (+) - for discussion see below.

The EBIC investigations in the volume of the sample were carried out either on bevels or after sufficient surface removal by etching. Al Schottky contacts were used for charge collection. λ and c_{max} were determined for a beam energy E_o = 30 keV thereby averaging over a sufficiently large area. The measurements were performed in bulk regions of constant density of EBIC contrasts, as for $z \gtrsim 150$ μm in Fig. 1. Thus, a homogeneous defect-density depth-distribution F(a) could be assumed.

The maximum contrast values c_{max} were near 0.3 in many cases. The size of the defects showing EBIC contrast was determined by TEM to be in the range of 1 μm or less so that they could be considered as being small compared to R and treated as point-like defects. The bulk diffusion length L_B was determined from energy-dependent EBIC measurements /9/.

The measured data (crosses) are shown in Fig. 9. For both calculated curves and measured data L_B increases with λ. More detailed information about two typical samples denoted A and B is given in Table 1.

(i) It is found that the total defect density obtained by etching (N_{OP} + N_{SF} + ...) is considerably larger than the density of defects giving EBIC contrast N_E, but N_{SF} and N_E are usually in the same order of magnitude.

(ii) In sample A $L_E < L_M$ is observed, i. e., the dominant source of bulk recombination are defects showing EBIC contrast, probably stacking faults (SF). Sample B has $L_E \simeq L_M$, again indicating a significant contribution to bulk recombination by defects with EBIC contrast.

(iii) The diffusion length between the contrast sites, L_M, is estimated to be smaller than the diffusion length in the denuded zone L_{DZ} for both samples.

In the light of our results defects showing EBIC contrasts, i. e., mainly SF, are the essential sources of

---

Table 1. Characteristics of samples A and B as obtained by etching and EBIC

sample	Wright etching		EBIC				calculated* using (1) and (2)	
	N_{OP} (cm^{-3})	N_{SF} (cm^{-3})	N_E (cm^{-3})	c_{max}	L_B (μm)	L_{DZ} (μm)	L_M (μm)	L_E (μm)
A	10^{10}	6×10^{9}	3×10^{9}	0.3	5.5	30	11	6.3
B	10^{9}	1×10^{8}	2×10^{8}	0.3	14	30	20	20

N_{OP}, N_{SF} : densities of oxygen precipitates (OP) and stacking faults (SF), respectively, determined by Wright etching,
N_E : density of EBIC contrasts at E_o = 30 keV,
L_{DZ} : diffusion length in the denuded zone of the wafer determined by the method given in /3/.

* L_E was calculated by relation (2) using $f_{max}(L_M = 100\ \mu m, \ldots) = 0.027\ \mu m^{-1}$ for both samples. L_M = 20 μm was found for sample B by inserting L_E = 20 μm and L_B = 14 μm in relation (1) resulting in a slightly reduced f_{max} value only, compare Fig. 4. For sample A, however, with L_M = 11 μm the corresponding value $f_{max}(L_M = 11\ \mu m, \ldots) \simeq 0.025\ \mu m^{-1}$ is smaller. Consequently a correction of f_{max} would result in a small decrease of L_E but in an increase of L_M. For considerably smaller L_M values such corrections could be of more significance.

bulk recombination in intrinsically gettered p-type Cz silicon. Possibly, recombination activity of SF is caused by precipitates decorating the Frank partial dislocations. In contrast to /6/ individual oxygen precipitates (OP) cannot be considered to play the dominant role in bulk recombination although they might be responsible for the enhanced recombination background in the bulk as compared to the recombination in the denuded zone ($L_M < L_{Dz}$). Dominant OP recombination seems to be rather confined to samples with very high OP densities $N_{OP} \sim 10^{12}...10^{13}$ cm^{-3} /6/ produced by long-duration heat treatments not typical of normal IG procedures.

Conclusions

In conclusion we can state that a detailed analysis of EBIC diffusion-length and contrast data allows one to estimate to which extent the average diffusion length is determined by recombination-active defects showing EBIC contrast, and may be used to identify essential sources of bulk recombination in annealed silicon. Investigations on the relationship between diffusion length and defect densities as found by EBIC have been carried out earlier by various authors /1,7,14/, but without considering the values of the EBIC contrasts.

Taking into account also the EBIC contrasts of the defects, i.e., their respective recombination strength, we were able to get an improved description of defect accumulations and their effect on recombination properties.

Further improvements might be possible by utilizing the whole EBIC distribution in the area where the diffusion length is measured, requiring additional efforts for image analysis, however.

Acknowledgements

The authors would like to thank Dr. C. Donolato for critical reading of the manuscript. Further we are grateful to Mr. A. Seyfarth for numerical calculations concerning validity of relation (8) and to Mrs. K. Peters for typing the manuscript.

References

/1/ Castaldini A, Cavallini A, Cavalcoli C.(1987). EBIC diffusion length of dislocated silicon. Preprint Proc. 5th Oxford Conference on Microscopy of Semiconductor Materials. Inst. of Physics, U.K.

/2/ Donolato C. (1978/79). On the theory of SEM charge-collection imaging of localized defects in semiconductors. Optik 52, 19-32.

/3/ Donolato C, Kittler M. (1988). Depth profiling of the minority-carrier diffusion length in intrinsically gettered silicon by electron-beam-induced-current. J. Appl. Phys. 63, 1569-1579.

/4/ Donolato C, Klann H. (1980). Computer simulation of SEM electron beam induced current images of dislocations and stacking faults. J. Appl. Phys. 51, 1624-1633.

/5/ Everhart TE, Hoff PH. (1971). Determination of kilovolt electron energy dissipation vs penetration distance in solid materials. J. Appl. Phys. 42, 5837-5848.

/6/ Hwang JM, Schroder DK. (1986). Recombination properties of oxygen-precipitated silicon. J. Appl. Phys. 59, 2476-2487.

/7/ Inoue N, Wilmsen CW, Jones KA. (1981). The effects of intragrain defects on the local photoresponse of polycrystalline silicon solar cells. Solar Cells 3, 35-43.

/8/ Kittler M, Richter H, Seifert W. (1987). Influence of intrinsic gettering on silicon recombination properties and their relation to device performance. Proc. 17th European Solid State Device Research Conference "ESSDERC", Bologna - Italy, Sept. 1987, p. 343-346.

/9/ Kittler M, Schröder K.-W.(1983). Determination of semiconductor parameters and of the vertical structure of devices by numerical analysis of energy-dependent EBIC measurements. Phys. Stat. Sol.(a) 77, 139-151.

/10/ Kittler M, Seifert W, Donolato C. (1987). Minority-carrier diffusion-length depth distribution in intrinsically gettered silicon and its influance on device performance. Proc. 2nd Intern. Autumn Meeting "GADEST". Garzau (G.D.R.), 11-17 October 1987 (Ed). H. Richter. Academy of Sciences of the G.D.R., p. 341-346.

/11/ Kittler M, Seifert W. (1981). On the sensitivity of the EBIC technique as applied to defect investigations in silicon. Phys. Stat. Sol. (a), 66, 573-583.

/12/ Kittler M, Seifert W. (1981). On the characterization of individual defects in silicon by EBIC. Crystal Research and Technology 16, 157-162.

/13/ Pasemann L, Blumtritt H, Gleichmann R. (1982). Interpretation of the EBIC contrast of dislocations in silicon. Phys. Stat. Sol. (a) 70, 197-209.

/14/ Pizzini S, Bigoni L, Beghi M, Chemelli C. (1986). On the effect of impurities on the photovoltaic behaviour of solar grade silicon. J. Electrochem. Soc. 133, 2363-2373.

/15/ Richter H. (1985). Gettering in the silicon device technology. Proc. 1st "GADEST". Garzau (G.D.R.), Oct. 1985. (Ed.) H. Richter. Acad.Scie.GDR, p. 1-20.

/16/ Schroder DK. (1984). Effective lifetimes in high quality silicon devices. Solid-State Electronics 27, 247-251.

/17/ Wu CJ, Wittry DB. (1978). Investigation of minority-carrier diffusion lengths by electron bombardment of Schottky barriers. J. Appl. Phys. 49, 2827-2836.

Discussion with Reviewers

C. Dimitriadis: You determined L_B from energy-dependent charge collection measurements $\eta(E_0)$ of Schottky barriers. In this method various parameters are involved. Some of the parameters of the method, beam penetration depth (ξ) for instance, are not well known. In a paper from Watanabe et al. (IEEE Trans. Electr. Dev. ED-24, 1172, 1977) I calculate $\xi \simeq 2.9$ µm at $E_0 = 35$ keV, whereas in a paper from Valkealathi and Nieminen (Appl. Phys. A 32, 95, 1983) two sets of parameters for the equation $\xi = \alpha(E_0)^n$ are offered, yielding $\xi = 3.9$ µm and $\xi = 4.3$ µm at $E_0 = 35$ keV, respectively. How do errors in these parameters affect the values of L_B obtained from measurements by the method and, also, the conclusions concerning the identification of the essential sources of bulk recombination in the material?

Authors: Some discussion concerning the influence of errors in the collection efficiency η and of errors in other parameters on the diffusion length L has been published, see M. Kittler, W. Seifert, K.-W. Schröder, E. Susi in Crystal Res. Technol. 20, 1435 (1985). As to the particular effect of errors in beam penetration, it is clear that larger (smaller) values for the electron range R would result in an overestimation (underestimation) of L.

In our analysis of the experimental $\eta(E_0)$ data (see text reference /9/) we describe the beam penetration by expressions published by Everhart and Hoff (see text reference /5/). At $E_0 = 35$ keV, for instance, one obtains

$R = 0.0171 \times 35^{1,75}$ µm $\simeq 8.6$ µm.

This description coincides quite well with new results on beam penetration in silicon, see U. Werner, F. Koch, G. Oelgart in J. Phys. D: Appl. Physics 21, 116 (1988).

Furthermore, a good correspondence is found between L values obtained from spatial decay measurements $I_{EBIC}(x)$ and L values determined by $\eta(E_0)$ measurements (M. Kittler, W. Seifert, H. Richter in Izv. AN SSR, Seria Fizicheskaya 51, 155 (1987)). Consequently the L_B values given in this paper seem to be reliable so that no problems concerning identification of the essential sources of bulk recombination are expected.

J. Heydenreich: The suggestion of the authors to regard the average bulk diffusion length (L_B) to consist of a contribution by point defects and crystal defects without EBIC contrasts (L_M) and a contribution by the observed defects with EBIC contrasts (L_E) seems to be a useful proposal of a classification. In practice, however, difficulties may arise with the question to what extent a defect (crystal defect) exhibits an EBIC contrast, or not, depending both on the defect type and on the experimental measurement technique used. To avoid arbitrariness in the classification, additional criteria should be taken into account. What are your suggestions with respect to this?

Authors: Some arbitrariness in defect classification may be due to the minimum contrast c_{min} still detectable which is mainly determined by the sensitivity of the EBIC electronics used, see e. g., text reference /11/. However, c_{min} has small influence to L_E only, so that relation (2) (not containing c_{min}) can be used in practice for L_E determination. Consequently no additional criteria are needed for samples with contrast values well above c_{max}.

D. Ioannou: The analysis provided in this paper rests on the equality of the two contrasts c and c* (eq. 8). This equality, however, is not obvious, and the authors are asked to justify it at some length.

Authors: The definition of c* is

$$c^* = 1 - \frac{I_d^*}{I_0^*} \qquad (D1)$$

where I_d^* and I_0^* can be written, see eq. (7), as:

$$I_d^* = I_0 (1 - \gamma f_d^*) \qquad (D2)$$

$$I_0^* = I_0 (1 - \gamma f_0^*) \qquad (D3)$$

with

$$f_{d/0}^* = f_{d/0} + \sum_{i=1}^{N} \frac{\gamma_i}{\gamma} f_{i\,d/0} = f_{d/0} + \Delta f_{d/0} \qquad (D4).$$

Using $f_d^* = f_d + \Delta f_d$ for (D2), and taking into account that

$$(1 - \gamma f_d - \gamma \Delta f_d) \simeq (1 - \gamma f_d)(1 - \gamma \Delta f_d)$$

one obtains

$$I_d^* \simeq I_0 (1 - \gamma f_d)(1 - \gamma \Delta f_d) \qquad (D5).$$

Inserting relation (D3) now in (D5) one gets

$$I_d^* \simeq I_o^*(1-\gamma f_d)\frac{(1-\gamma A f_d)}{(1-\gamma f_o^*)} = I_o^*(1-\gamma f_d)M \quad (D6).$$

From numerical calculations M is found to be close to 1 at defect distances $\lambda > 2R$ and for small γ values. (For defects arranged as a cubic lattice, $R = 6$ µm, and $L_M = 100$ µm this is true for defect strengths $\gamma < 11$ µm which correspond to EBIC contrasts $c < 0.3$.) Using $M \simeq 1$ one obtains from (D6) after permutation

$$\gamma f_d \simeq 1 - \frac{I_d^*}{I_o^*} \quad (D7).$$

Finally, considering $c = \gamma f_d$ and (D1) we have as result $c \simeq c^*$ (8).

C. Dimitriadis: Based on the assumption of homogeneous defect density depth-distribution it is concluded that, for closely neigboured defects and for usual c_{min}/c_{max} ratios the relation (2) may be used for estimation of L_E. Is the above conclusion still true if the defect density depth-distribution is non-homogeneous?

J. Heydenreich: The assumption of the paper that with respect to visible defects all recombination centres located at the defects are homogeneously distributed was used as a simplification for the calculations. Did you also employ other (more or less idealized) assumptions of this simplification on your results?

Authors: The estimation of the L_E component is based on the important assumption that the effect of recombination-active defects can be approximated by recombination at homogeneously distributed recombination centres. However, this assumption should become progressively unreal for increasing distances between the defects and for pronounced defect depth-profiles. So it is not possible to definitely answer the question about the influence of non-homogeneous depth distributions up to now. Therefore, numerical calculations should be made, comparing the mean EBIC signal in a given area obtained for centres concentrated at individual defects with the EBIC calculated for an identical number of centres but being homogeneously distributed under the regarded area.

C. Dimitriadis: The authors should discuss the following point: According to the analysis the range of depth (Δa) where defects can be detected is related to the electron range R (see Fig. 8). For defects of high contrast ($c_{min}/c_{max} \ll 1$) $\Delta a > R$, i. e., by increasing the electron range R the information range Δa increases. On the other hand, the EBIC resolution is only determined by the generation volume (C. Donolato, Appl. Phys. Lett. 34, 80, 1979). Therefore, an appropriate electron beam energy should be used to achieve good resolution and obtain large information range Δa.

Authors: It is true that EBIC resolution and consequently smallest measurable λ values are determined by the beam energy E_o or the electron range R, respectively. For $E_o = 30$ keV the smallest λ values measured are in the range of $R \simeq 6$ µm, compare Fig. 9. When decreasing R, both λ and Δa decrease and the information range moves towards the Schottky depletion-region. With continuous reduction of R, information range and depletion region begin to overlap partially. Our estimations based on Donolato's contrast model (see text reference /2/) become wrong then, because this model does not consider defects inside the depletion-region, where drift processes are dominant.

In silicon having a resistivity of 10...20 ohm×cm, as used in our experiments, the depletion-layer width is around 0.5 µm. Under these conditions, use of at least $E_o = 30$ keV or $R \simeq 6$ µm, respectively, for measurements permits to neglect depletion layer effects. Larger beam energies could be used for samples having sufficiently large λ values.